The meltwater Retention Model Intercomparison Project (RetMIP): Evaluation of nine firn models at four weather station sites on the Greenland ice sheet

Supplementary Material

Baptiste Vandecrux[1,2], Ruth Mottram[3], Peter L. Langen[3], Robert S. Fausto[1], Martin Olesen[3], C. Max Stevens[4], Vincent Verjans[5], Amber Leeson[5], Stefan Ligtenberg[6], Peter Kuipers Munneke[6], Sergey Marchenko[7], Ward van Pelt[7], Colin Meyer[8], Sebastian B. Simonsen[9], Achim Heilig[10], Samira Samimi[11], Horst Machguth[12], Michael MacFerrin[13], Masashi Niwano[14], Olivia Miller[15], Clifford I. Voss[16], Jason E. Box[1]

[1] Geological Survey of Denmark and Greenland, Copenhagen, Denmark.
[2] Department of Civil Engineering, Technical University of Denmark, Lyngby, Denmark.
[3] Danish Meteorological Institute, Copenhagen, Denmark
[4] Department of Earth and Space Sciences, University of Washington, WA USA
[5] Lancaster Environment Centre, Lancaster University, Lancaster, UK
[6] IMAU, Utrecht University, The Netherlands
[7] Department of Earth Sciences, Uppsala University, Uppsala, Sweden
[8] Thayer School of Engineering, Dartmouth College
[9] National Space Institute, Technical University of Denmark, Kgs. Lyngby, Denmark
[10] Department of Earth and Environmental Sciences, LMU, Munich, Germany
[11] Department of Geography, University of Calgary, Calgary, AB, Canada
[12] Department of Geosciences, University of Fribourg, Switzerland
[13] Cooperative Institute for Research in Environmental Sciences, University of Colorado, Boulder, CO, USA
[14] Meteorological Research Institute, Japan Meteorological Agency, Tsukuba, 305-0052 Japan
[15] U. S. Geological Survey, Utah Water Science Center, Salt Lake City, UT, USA
[16] U. S. Geological Survey, Menlo Park, CA, USA

Correspondence to: B. Vandecrux (bav@geus.dk)

Supplementary Text S1: Specific notes related to the models

Darcy-like runoff routine in the GEUS model

While the firn model from Vandecrux et al. (2018, 2020) did not allow runoff from the firn, we here implemented a novel runoff scheme that considers that available water (beyond irreducible water content) may exit the model column based on the local surface slope and simulated firn characteristics. We adjoin to our modelled firn column an identical virtual neighbor and consider that the two columns are inclined an angle equal to the site's surface slope (Table 4, Figure ST1a). The excess water is then allowed to move away from the modelled firn column, into the corresponding layer of the virtual column based on Darcy's law. (Figure ST1b). Darcy's law makes the water flux to the downstream neighbor dependent on the surface slope, the amount of water available and on each layer's hydraulic conductivity.

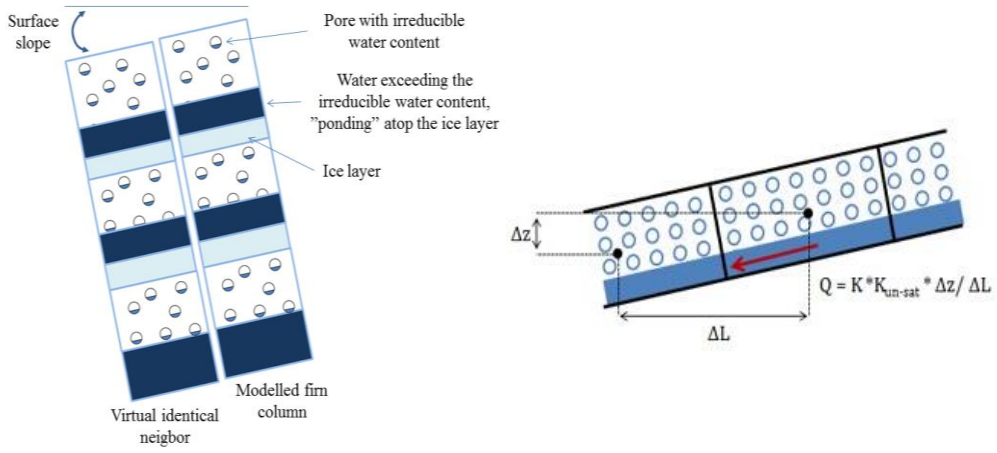

Figure ST1. Illustration of the runoff calculation in the GEUS model. The modelled firn modelled is agjoined a virtual twin and the two are inclined according to the surface slope. The water flux out of the main column into the virtual neighbor can thereafter be calculated based on each layer's hydraulic conductivity, water content and surface slope.

Adaptation of the surface forcing in the MeyerHewitt model

In Meyer and Hewitt (2017), we use a simplified snow permeability κ as a function of the porosity φ, which is given by

$$\kappa = \frac{d_p^2}{180}\phi^3,$$

where d_p is the snow grain size and 180 is an empirical constant. Here we use the full Carman-Kozeny permeability, which is given by

$$\kappa = \frac{d_p^2}{180}\frac{\phi^3}{(1-\phi)^2}$$

and take $d_p = 10^{-4}$ m.

For RetMIP, the temperature and melt rate are given at the the surface. This is a different type of boundary condition than is implemented in Meyer and Hewitt (2017), which instead requires a surface energy flux and *computes* the surface temperature and/or melt rate. To account for this, we derive an (approximate) equivalent surface energy flux from the given temperature and melt rate. The model-computed temperature and melt rate are then not exactly the same as those given but are most of the time very close. Starting from equation (15) in Meyer and Hewitt (2017), the surface energy balance is

$$\rho_i c_p (1-\phi)(w_i - z_s)(T - T_m) - K\frac{\partial T}{\partial z} = -Q + h(T - T_m) + \rho_w \mathscr{L} M.$$

We estimate that the first (advective) term and the second (conductive) term are relatively small in this equation, with the dominant balance being between the terms on the right: the prescribed flux Q, the parameterised surface-air heat exchange $h(T - T_m)$, and the latent heat of melting $\rho_w L\, M$. The smallness of the first two terms is reflected by the relatively large Stefan number S and the Péclet number Pe, defined in Meyer and Hewitt (2017). We note however that the conductive term may be important in situations of rapidly changing temperature, and this accounts for the differences between our model-derived surface temperature and the prescribed values shown in figure 1 below. Neglecting the terms on the left we have

$$Q \approx h(T - T_m) - \rho_w \mathscr{L} M,$$

and we use this to infer the equivalent energy flux $Q(t)$ to be used as the input to our model code, from the given time series of T and M. In figure ST2, we compare the given surface temperature input to the surface temperature output by the code. The agreement is mostly good, which validates the method for computing the surface forcing.

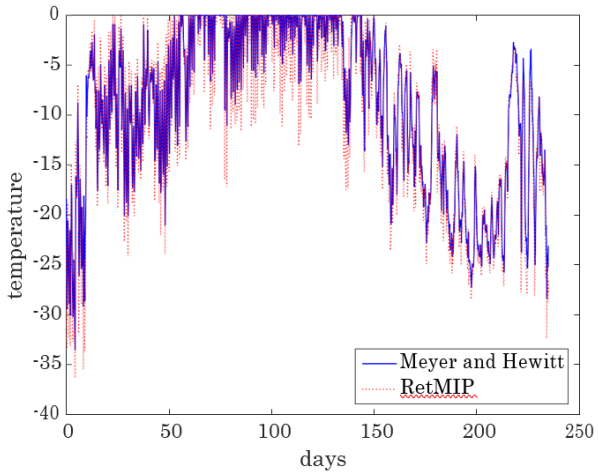

Figure ST1: Comparison between input surface temperature from RetMIP and output surface tem- perature from the Meyer and Hewitt (2017) code. The two temperatures agree quite well, although the code output surface temperatures have a smaller amplitude than the RetMIP inputs.

Supplementary Text S2: Additional information about weather stations at Dye-2 and FA sites

Weather station at Dye-2 used for the 2016 melt season

The weather station used for the Dye-2_16 test case was installed by Samira Samimi and Shawn Marshall in spring 2016. It had for objective to resolve the full surface energy budget and to observe the meltwater percolation and retention in the snow using Time Domain Reflectometry as already done in alpine snowpack (Samimi and Marshall, 2017). The station was installed next to the upward-looking radar (Heilig et al., 2018). Measurements of temperature and humidity was done using a Campbell Scientific HC-S3-XT, upward/downward shortwave/longwave radiation with Kipp and Zonen CNR1, wind speed and direction with a RM Young 05103, air pressure with RM Young 61250V, and snow surface height were made every 10 seconds, with 30-minute averages recorded on the datalogger. An SR50 ultrasonic sensor is used to monitor the snow-surface height. All these sensors were connected to a Campbell Scientific CR1000 datalogger.

Weather station at FA site

FA station, also referred as S21, is located 66°22' N, 39°19' W and ~1663 m a.s.l.. Air temperature and relative humidity are measured by a Vaisala HMP35AC, air pressure by a Vaisala PTB101B, wind speed and direction are observed using a Young 05103, and the radiative fluxes (shortwave and longwave fluxes) by a naturally-ventilated Kipp and Zonen CNR1 radiometer. The tilt of the AWS mast in two perpendicular directions is observed using homemade inclinometers. Surface height is measured using a sonic height ranger. The initial height of the wind and air temperature sensors was 3.80m above the surface. All quantities are sampled every 6 min, and hourly averages are recorded by a Campbell CR10X datalogger.

Supplementary Figures:

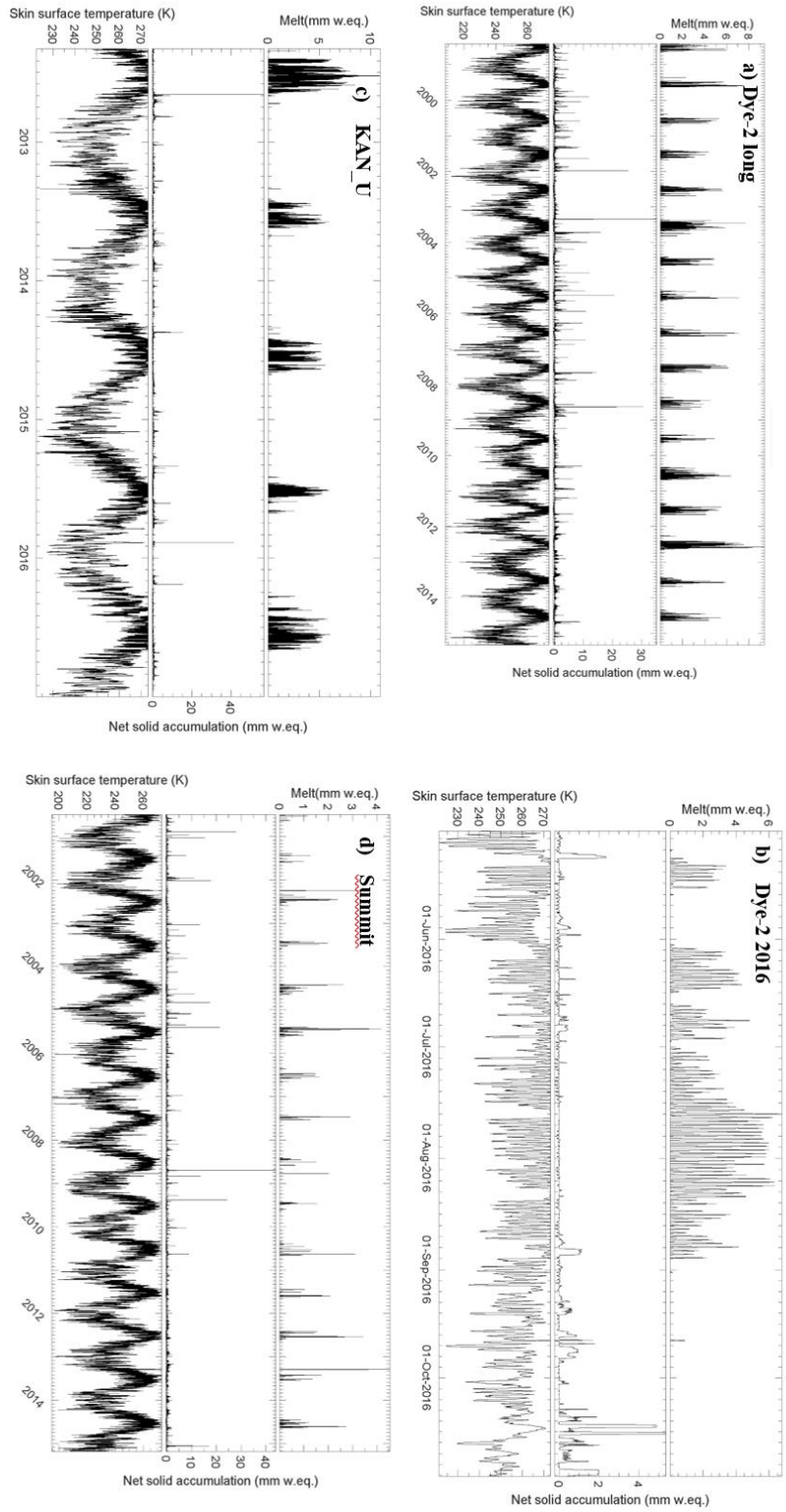

Figure S1. Surface forcing given to all firn models at Dye-2 for the 1998-2015 period (a) and for the 2016 summer (b), at KAN_U for 2012-2017 (c), at Summit for 2000-2015 (d) and at FA for May-Nov. 2014 (e).32

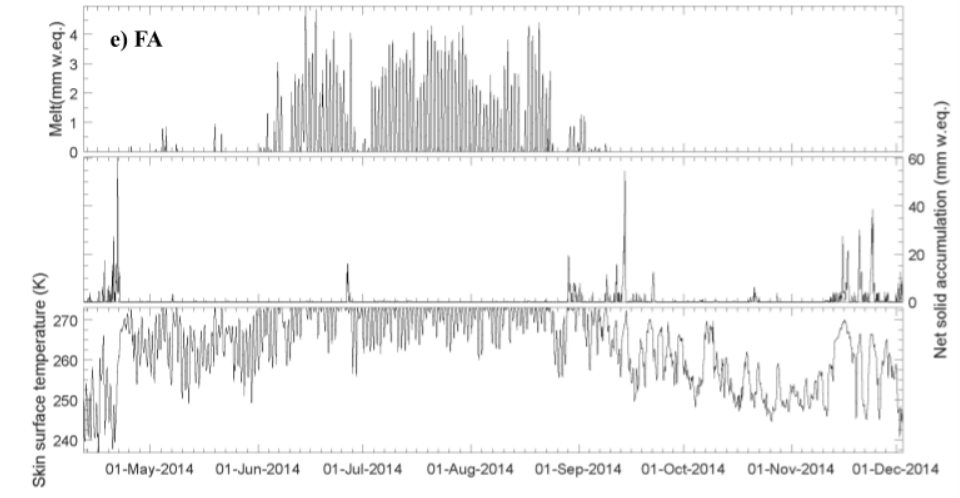

Figure S1. (continued)

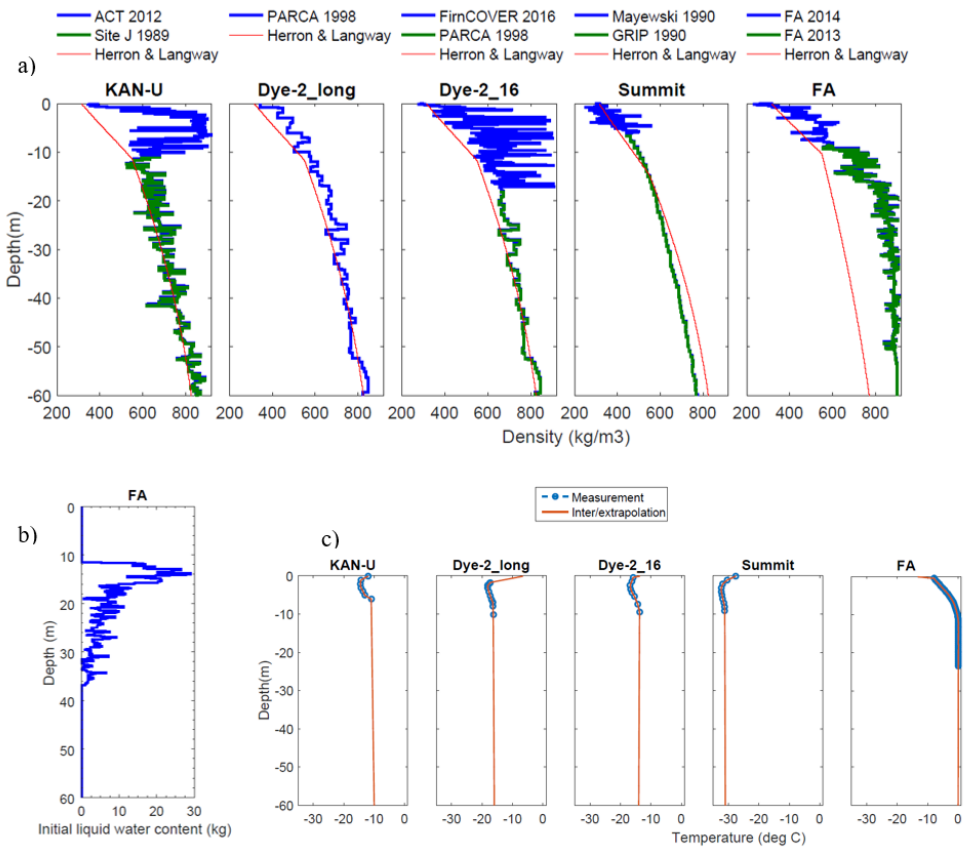

Figure S2. a) Initial firn density imposed to all models. b) Initial liquid water content imposed to all models at the FA site. c) Initial firn temperature profile imposed to all models.

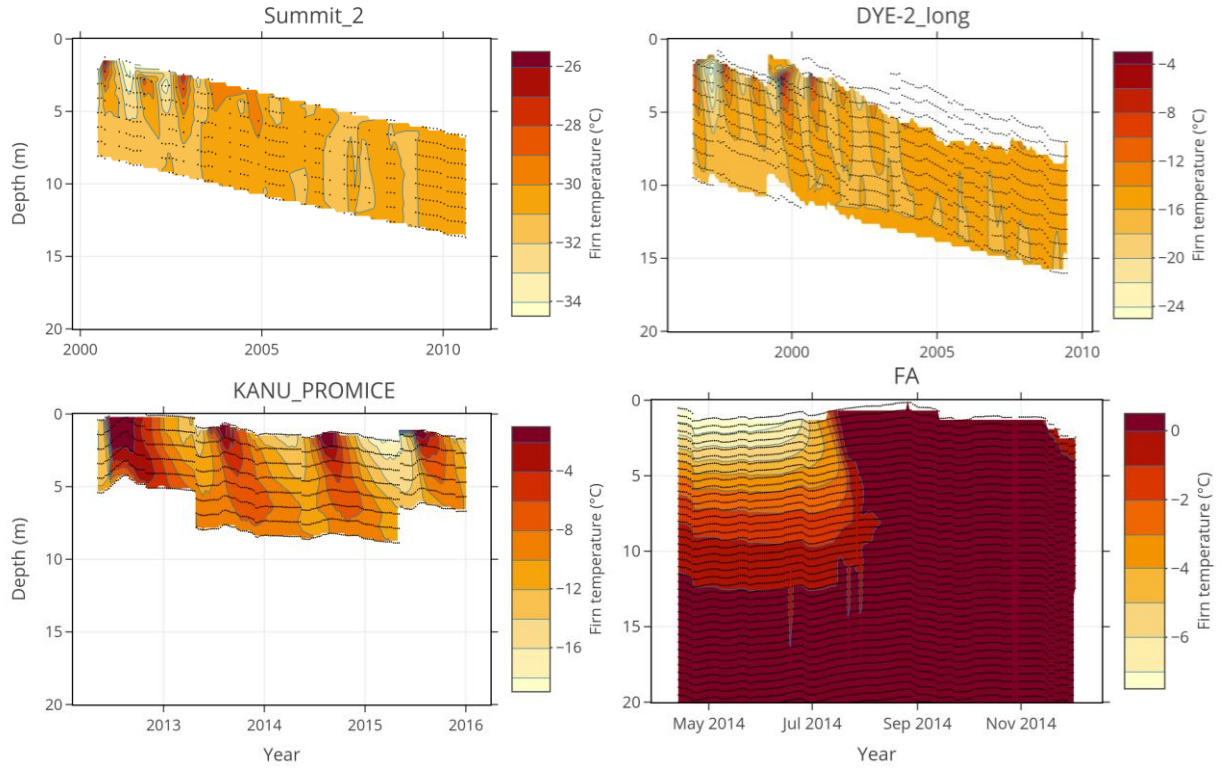

Figure S3. Firn temperature observations and thermistor depth.

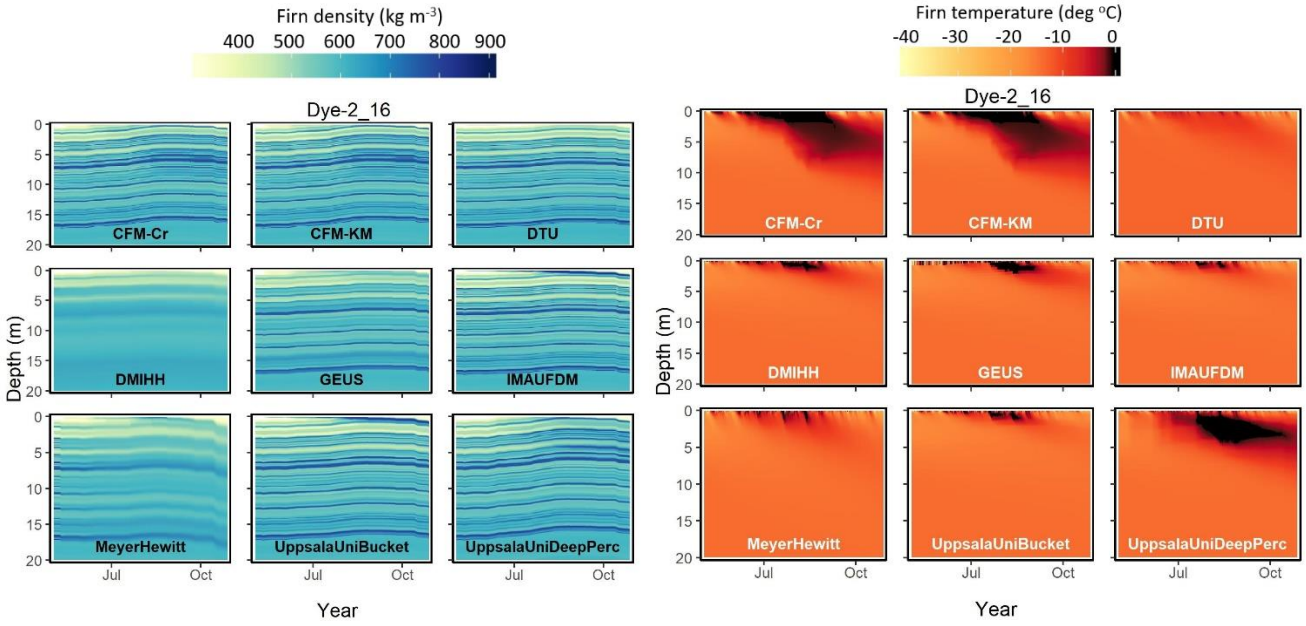

Figure S4. Simulated firn density and temperature at Dye-2_16.

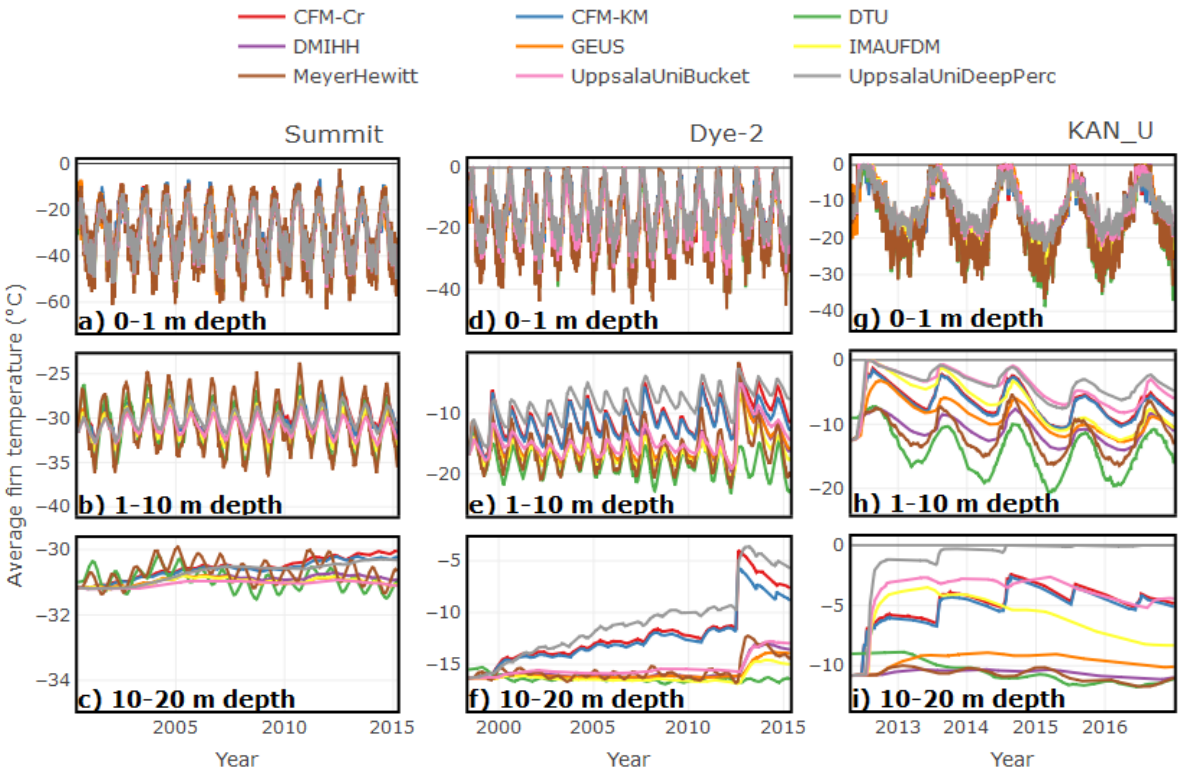

Figure S5. Modelled average firn density for the top 1 m (a,d,g), for the 1-10 m depth range (b,e,h) and 10-20 depth range (c,f,i) at Summit (a,b,c), Dye-2 (d,e,f) and KAN_U (g,h,l).

Table S1. Weather data availability, in %, at Summit, KAN_U and Dye-2 station

	Summit	KAN_U	Dye-2_long
Air temperature	92.1	99.9	88.4
Downward shortwave radiation	84.2	74.1	87.4
Air pressure	85.9	100.0	33.0
Relative humidity	89.6	100.0	70.7
Wind speed	84.2	99.8	81.9
Downward longwave radiation	0.0	99.7	0.0

Table S2. Firn density profiles used for validation.

KAN_U	
core_1_2013	
core_2_2013	Machguth et al. (2016)
core_1_2015	
core_1_2016	MacFerrin et al. (2019)
core_2_2016	
Dye-2	
ACT11D	Forster et al. (2014)
core_5_2013	Machguth et al. (2016)

core_6_2013	
core_11_2015	Vandecrux et al. (2018)
Summit	
Albert_2000	Albert and Schultz (2002)
Albert_2007	Lomonaco et al. (2011)
core_22_2015	Vandecrux et al. (2018)
core_23_2015	
core_24_2015	
core_25_2015	